

Supporting Information

Ultrathin MOF Nanosheet-based Resistive Gas Sensors for Highly Sensitive Detection of Methanol at Room Temperature

By Fangna Dai,^{†,1} Xiaoya Cui,^{†,3} Yuwei Luo,¹ Dongzhi Zhang,¹ Nanjun Li,² Ying Huang,⁴

Yongwu Peng^{,2}*

[†]These authors contributed equally to this work.

¹ School of Materials Science and Engineering, China University of Petroleum (East China), 66 Changjiang West Road, Qingdao, Shandong 266580, China

² College of Materials Science and Engineering, Zhejiang University of Technology, Hangzhou, 310014, China.

E-mail: ywpeng@zjut.edu.cn

³ Ministry of Education Key Laboratory of Protein Sciences, Beijing Advanced Innovation Center for Structural Biology, School of Life Sciences, Tsinghua University, Beijing 100084, China.

⁴ State Key Laboratory of Environment-friendly Energy Materials, Southwest University of Science and Technology, Mianyang, 621010, PR China

Experimental Section

Materials. The H₆TCPP ligand, CoCl₂·6H₂O, HClO₄ and Polyvinyl pyrrolidone (PVP, MW = 40,000) were purchased from Sigma-Aldrich. Ethanol, Methanol (99.9%) was purchased from Merck. Dimethylacetamide (DMA) was purchased from Fisher Scientific. All the chemicals were used as received without further purification.

Synthesis of Co-TCPP-AC bulk crystals. CoCl₂·6H₂O (10.0 mg, 0.042 mmol), H₆TCPP (10.0 mg, 0.013 mmol), DMA (1.0 mL) and HClO₄ (50 μL) were heated to 120 °C for 24 h in a sealed tube. The red crystalline block formed on the walls of the glass tube was collected by filtration, washed with DMA and ethanol and dried in air (yield: 70%, based on cobalt). Elemental analysis calcd (%): C, 57.10; H, 3.50; N, 6.29; found (%): C, 57.41; H, 3.98; N, 6.64.

Synthesis of Co-TCPP-AC NSs. CoCl₂·6H₂O (5.0 mg, 0.021 mmol), H₆TCPP (2.5 mg, 0.006 mmol), DMA (10.0 mL), HClO₄ (25 μL) and PVP (10.0 mg, MW = 40,000) were heated to 120 °C and kept for 6 h in a sealed tube, and then cooling down to 25 °C over 10 h. The yield of Co-TCPP-AC NSs is about 2.25 mg (45% based on cobalt).

Characterization. Transmission electron microscopy (TEM) measurement, high resolution TEM (HRTEM), dark-field scanning TEM-energy dispersive X-ray spectroscopy (DF-STEM-EDS) and elemental mappings were performed on JEOL JEM2100F microscope operated at 200 kV. Selected area electron diffraction (SAED) patterns were recorded on JEOL JEM-2010UHR operated at 200 kV. X-ray diffraction (XRD) patterns were recorded with a Panalytical X-ray diffractometer, using Cu-Kα radiation (λ=1.5406 Å). The thickness of nanosheets was measured by atomic force microscopy (AFM, Cypher, Asylum Research). The ultraviolet photoelectron spectroscopy (UPS) tests were conducted on a Thermo Scientific ESCALAB 250 Xi XPS system.

X-ray Structural Studies. Crystals of complex Co-TCPP-Ac with appropriate dimensions were quickly mounted on a glass fiber under an optical microscope. X-ray diffraction data were collected on an Agilent Xcalibur Eos Gemini diffractometer with Cu-K α radiation ($\lambda = 1.54178$ Å) at 273 K. Absorption corrections were applied using the multi-scan method. All structures were solved by direct methods and refined by full-matrix least-squares on F^2 using *SHELXS-97*. All non-hydrogen atoms were located from iterative examination of difference F-maps and refined with anisotropic thermal parameters on F^2 . The organic hydrogen atoms were placed in calculated positions and refined as riding atoms with isotropic displacement parameters 1.2-1.5 times U_{eq} of the attached atoms. The free solvent molecules in complex are highly disordered, and no satisfactory disorder model could be achieved. The *PLATON/SQUEEZE* routine was used to remove scattering from the disordered solvent molecules. Pertinent crystallographic data collection and refinement parameters are collected in Table S1. Crystallographic data have been deposited at the Cambridge Crystallographic Data Center (CCDC: 1426079). The data can be obtained from *CSD Communication*, 2022, DOI: 10.5517/ccdc.csd.cc1jvykw.

Table S1. Crystal Data for Co-TCPP-Ac.

Empirical formula	C ₅₀ H ₂₇ Co ₃ N ₄ O ₁₁
Formula weight	1036.52
Temperature/K	293K
Crystal system	orthorhombic
Space group	Cmmm
a/Å	17.5964(9)
b/Å	33.2980(10)
c/Å	16.5618(6)
α /°	90.00
β /°	90.00
γ /°	90.00
Volume/Å ³	9704.0(7)
Z	4
ρ_{calc} mg/mm ³	0.696
m/mm ⁻¹	0.537
F(000)	2052.0
Radiation	Cu K α ($\lambda = 1.54178$ Å)
2 θ range for data collection	3.58 to 51.38°
Index ranges	-15 \leq h \leq 21, -40 \leq k \leq 34, -15 \leq l \leq 19
Reflections collected	12003
Independent reflections	4913 [$R_{\text{int}} = 0.0982$, $R_{\text{sigma}} = 0.1315$]
Data/restraints/parameters	4913/0/163
Goodness-of-fit on F ²	0.774
Final R indexes [$I \geq 2\sigma(I)$]	$R_1 = 0.0683$, $wR_2 = 0.1738$
Final R indexes [all data]	$R_1 = 0.1335$, $wR_2 = 0.1985$

Fabrication of gas sensors. The sensing device is fabricated by using a planar rigid printed circuit board (PCB) as the substrate, a pair of Cu/Ni metal as interdigital electrodes (IDEs) and the Co-TCPP-Ac NS thin film as the active channel. Such device structure can ensure good attachment of the uniform and controllable Co-TCPP-Ac NS thin film to the electrodes, which can improve the sensitivity of the fabricated sensing devices. The electrode patterns are fabricated by using micro-nano fabrication techniques, including sputtering Cu/Ni thin films, lithography techniques and etching techniques. The Co-TCPP-Ac NS thin film was fabricated by spin-coating technique at 800 rpm for 30 s, followed by drying in oven at 60 °C for 3 h.

Gas sensor characterizations. The experiment was performed under specific conditions (30% RH) at 25°C. The gas-sensing properties of the sensor were investigated by exposing the devices

to various concentrations of methanol gas, ranging from 0.5 ppm to 100 ppm. The methanol gas sensing experimental device is shown in Fig. S5. The electrode was connected to a data logger (Agilent 34970A), which was used to record the corresponding resistance change of the sensors at 25 °C, via a RS-232 interface. The response (R), determined by $R = R_a/R_g$, was used for evaluating the sensing performances of sensors, where R_a and R_g were the measured resistance of the sensor in air and methanol gas, respectively. During a measurement, ambient air was used as the carrier gas and the electrodes were switched between air and methanol/air mixture to measure continuously, which were achieved by injecting a certain volume of methanol into a sealed container with a syringe. A stable baseline resistance was established in air, and a sharp decrease in resistance was observed within seconds upon exposing to dilute methanol vapor. The starting resistance level was recovered when the device is switched to air.

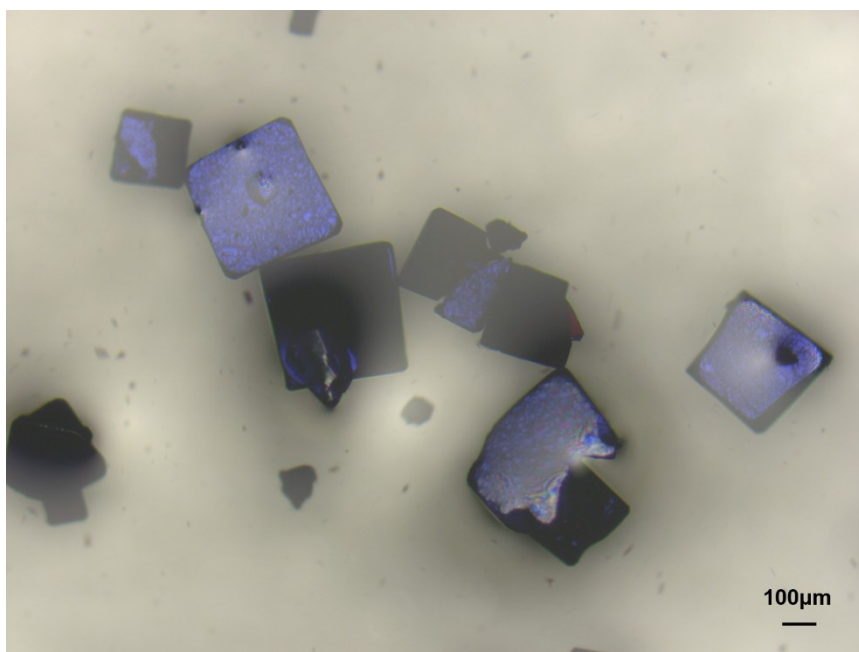


Fig. S1 Photos of Co-TCPP-Ac bulk crystals.

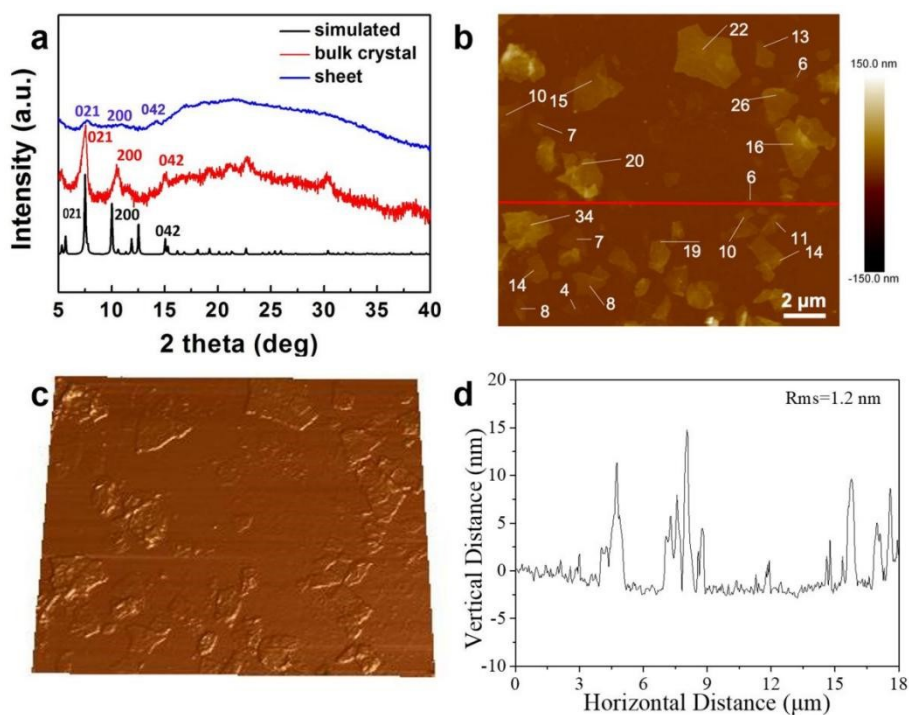


Fig. S2 (a) Experimental XRD patterns of Co-TCPP-Ac bulk crystals (black line), Co-TCPP-Ac NSs (red line) and the corresponding simulated XRD pattern (blue line). (b) AFM image of Co-TCPP-Ac NSs. The thickness of Co-TCPP-Ac NSs is marked in (b) with the unit of nm. (c,d) 3D image (c) and height profile (d) of the AFM image shown in (b).

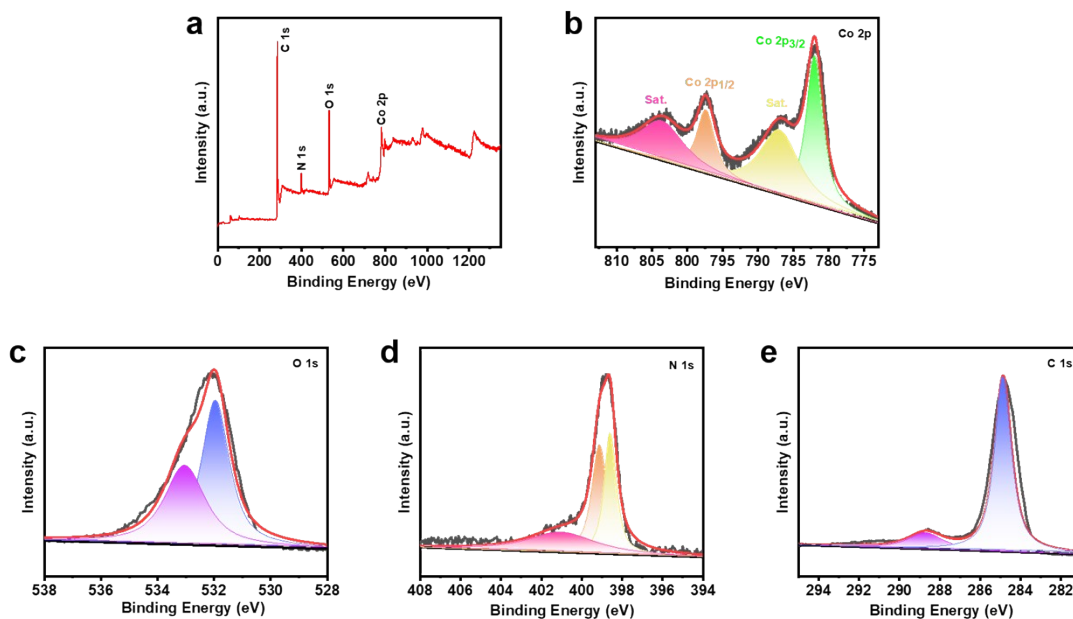


Fig. S3 The XPS spectrum of Co-TCPP-Ac NSs shows that the sample contains Co, O, C, N chemical elements (a). As shown in Fig b, the XPS spectrum of Co 2p can be divided into four peaks. The peaks at 781.6 eV and 797.4 eV are considered as Co 2p_{1/2} and Co 2p_{3/2}, respectively. The other two peaks (787.1 eV and 803.9 eV) are satellite peaks. In Fig c, the peaks of the O 1s XPS spectrum (533.1 eV and 531.1 eV) indicate that O in Co-MOF is metal oxide (Co-O) and carboxyl oxygen (O-C=O). The XPS spectrum of N 1s in Fig d can be split into three peaks at 398.6 eV, 399.1 eV and 401.1 eV, which can be assigned to pyridinic N (pyrid-N), =N- and -NH, respectively. In Fig e, the two peaks of the C 1s XPS spectrum at 288.8 eV and 284.9 eV can be regarded as carboxylate carbon (O-C=O) and benzene ring carbon (C=C).

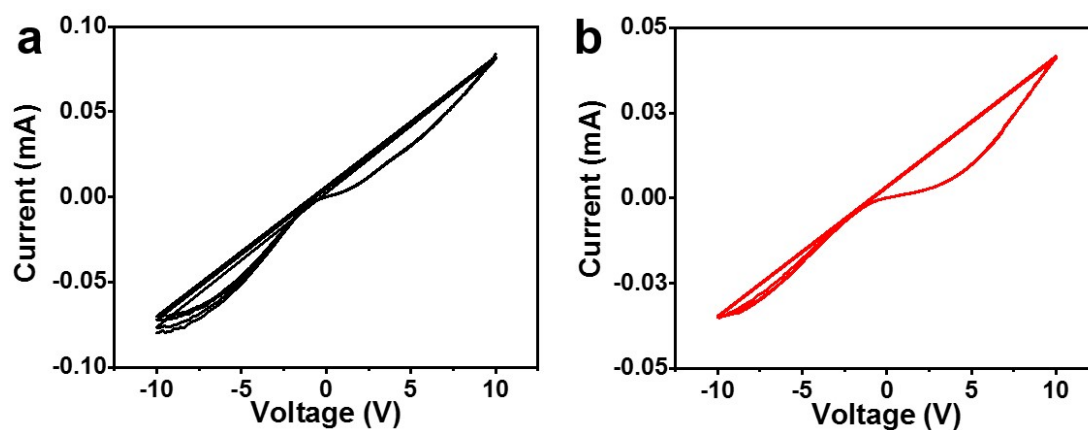


Fig. S4 Current (I) vs. voltage (V) plot for (a) Co-TCPP-Ac bulk crystals (black line) and (b) Co-TCPP-Ac NSs (red line).

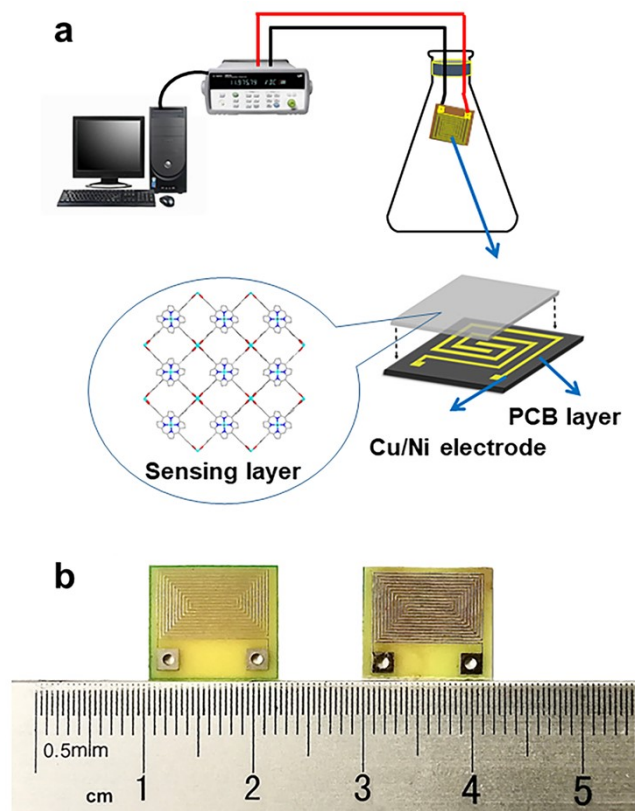


Fig. S5 (a) Schematic illustration of methanol gas sensing experimental setup. (b) The photograph of the fabricated sensing devices (before and after coating of Co-TCPP-Ac NSs film, respectively).

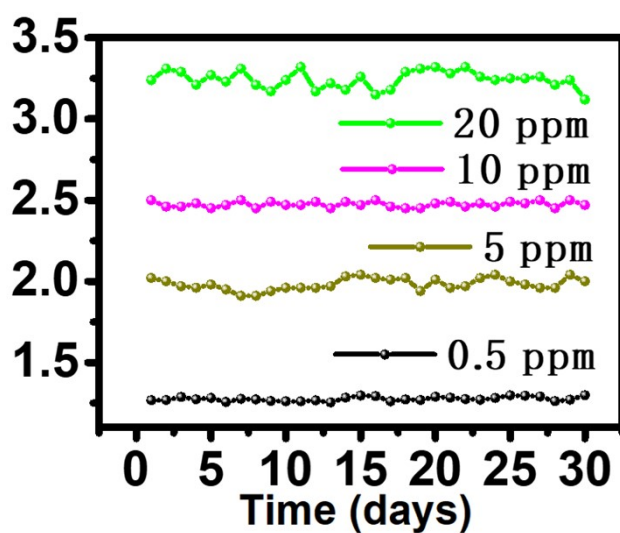


Fig. S6 Repeatability of the sensor in a testing period of 30 days under different concentrations of methanol, *i.e.*, 0.5, 5, 10, 20 ppm.

Table S2. Comparison of methanol gas sensors using different materials.

Materials	Fabricating technique	Working temperature	Gas Concentration (ppm)	Response R_a/R_g	Response/Recovery time	Ref.
Co-TCPP-Ac	Spin coating	25 °C	100	363.20	163 s / 7 s	This work
Al-ZnO	Spraying	275 °C	500	1.44	–	[1]
α -Fe ₂ O ₃ -HT	Coating	300 °C	100	9.10	5 s / 48 s	[2]
PtNP@POF-SiNWs	Depositing	25 °C	1200	13.50	–	[3]
NiO/Fe ₂ O ₃	Drop-coating	255 °C	100	107.90	0.1 s / 11.4 s	[4]
LaMg _{0.25} Ni _{0.75} O ₃	Spin coating	325 °C	40	1.27	–	[5]
In-doped NiO	Pressing	300 °C	200	10.90	273 s / 26 s	[6]
c-MWCNT/PANI	Pressing	25 °C	100	1.60	60 s / 90 s	[7]
n-ZnO/p-Si	Sputtering	100 °C	3	1.44	15 s / 18 s	[8]
rGO-TiO ₂	Depositing	110 °C	1	1.59	41 s / 46 s	[9]
Pd/RGO/TiO ₂	Depositing	50 °C	10	1.40	32 s / 30 s	[10]
GaN/Si	CVD	350 °C	500	2.50	8 s / 7 s	[11]
Co ₃ O ₄	Coating	220 °C	100	14.10	0.8 s / 7.2 s	[12]
AuNP/SnO ₂	Coating	200 °C	300	125.50	–	[13]
Gd _{0.9} Ca _{0.1} FeO ₃	Coating	260 °C	600	117.70	60 s / 66 s	[14]
SnO ₂ /Si-NPA	CVD	320 °C	10	3.60	4 s / 9 s	[15]

Table S3. Comparison of MOF as sensor toward different gases.

Materials	Sensor type	Working temperature	Gas concentration (ppm)	Response R_d/R_g	Response/Recovery time	Ref.
Co-TCPP-Ac	Resistance	25 °C	100 (CH₃OH)	363.20	163 s / 7 s	This work
Cu ₃ (HHTP) ₂	Resistance	25 °C	100 (NH ₃)	1.44	1.36 min / 9.11 min	[16]
MIL-53(Cr-Fe)/Ag/CNT	Resistance	25 °C	150 (CH ₃ OH)	1.34	10 min / 25 min	[17]
ZIF-67@SiNWs	Resistance	25 °C	10 (CH ₃ OH)	1.5	6 s / 36 s	[18]
SnO ₂ @ZIF-67	Resistance	205 °C	5 (CO ₂)	~1.82	~20 s / 22 s	[19]
ZnO@ZIF-8	Voltage	300 °C	100 (CH ₂ O)	4.00	16 s / 9 s	[20]
Ni-MOF-74	Impedance	25 °C	1 (CO)	40.20	–	[21]
MFM-300	Capacitance	25 °C	1 (SO ₂)	~16.00	–	[22]
NDC-Y-fcu-MOF	Capacitance	25 °C	1 (NH ₃)	~3.80	250 s / N.A.	[23]
[Cu(p-IPhHIDC)] _n	Impedance	25 °C	2 (NH ₃)	59.10	~10 min / ~10 min	[24]
Ba(o-CbPhH ₂ IDC)(H ₂ O) ₄ _n	Impedance	30 °C	25 (NH ₃)	25.30	~10 min / N.A.	[25]
HKUST-1	Impedance	25 °C	8 (p-xylene)	28.50	~150 s / ~150 s	[26]
Cu-BTC	Impedance	220 °C	500 (C ₂ H ₆ O)	~50.00	~2.4 min / ~2.4 min	[27]
TMA-Zn	Conductivity	25 °C	– (NH ₃)	~184.00	~60 min / N.A.	[28]

N.A. means there is no recovery time in the published paper.

References

- [1] P. P. Sahay, and R. K. Nath, *Sens. Actuators B Chem.*, 2008, **134**, 654.
- [2] W. Geng, S. Ge, X. He, S. Zhang, J. Gu, X. Lai, H. Wang, and Q. Zhang, *ACS Appl. Mater. Interfaces.*, 2008, **10**, 13702.
- [3] A. Cao, M. Shan, L. Paltrinieri, W. H. Evers, L. Chu, L. Poltorak, J. H. Klootwijk, B. Seoane, J. Gascon, and E. J. R. Sudhölter, *Nanoscale*, 2018, **10**, 6884.
- [4] W. Tan, J. Tan, L. Fan, Z. Yu, J. Qian, and X. Huang, *Sens. Actuators B Chem.*, 2018, **256**, 282.
- [5] S. Das, A. S. R. Murthy, K. I. Gnanasekar, and V. Jayaraman, *Sens. Actuators B Chem.*, 2018, **254**, 526.
- [6] C. Feng, X. Kou, B. Chen, G. Qian, Y. Sun, and G. Lu, *Sens. Actuators B Chem.*, 2017, **253**, 584.
- [7] A. Bora, K. Mohan, D. Pegu, C. B. Gohain, and S. K. Dolui, *Sens. Actuators B Chem.*, 2017, **253**, 977.
- [8] S. K. Sharma, B. Bhowmik, V. Pal, and C. Periasamy, *IEEE Sens. J.*, 2017, **17**, 7332.
- [9] D. Acharyya, S. Acharyya, K. Huang, P. Chung, M. Ho, and P. Bhattacharyya, *IEEE Trans Nanotechnol.*, 2017, **16**, 1122.
- [10] S. Ghosal, and P. Bhattacharyya, *Microelectron Reliab.*, 2017, **78**, 299.
- [11] H.-F. Ji, W.-K. Liu, S. Li, Y. Li, Z.-F. Shi, Y.-T. Tian, and X.-J. Li, *Sens. Actuators B Chem.*, 2017, **250**, 518.
- [12] W. Tan, J. Tan, L. Li, M. Dun, and X. Huang, *Sens. Actuators B Chem.*, 2017, **249**, 66.
- [13] T.-L. Han, Y.-T. Wan, J.-J. Li, H.-G. Zhang, J.-H. Liu, X.-J. Huang, and J.-Y. Liu, *J. Mater. Chem. C.*, 2017, **5**, 6193.
- [14] X. Wang, W. Ma, K. Sun, J. Hu, and H. Qin, *J. Rare Earths.*, 2017, **35**, 690.
- [15] L. L. Wang, Z. J. Li, L. Luo, C. Z. Zhao, and L. P. Kang, *J. Alloys Compd.*, 2016, **682**, 170.
- [16] M. S. Yao, X. J. Lv, Z. H. Fu, W. H. Li, W. H. Deng, G. D. Wu, and G. Xu, *Angew. Chem. Int. Ed.*, 2017, **129**, 16737.
- [17] M. Ghanbarian, S. Zeinali, and A. Mostafavi, *Sens. Actuators B Chem.*, 2018, **267**, 381.
- [18] Y. Qin, X. Wang, and J. Zang, *Chem. Phys. Lett.*, 2021, **765**, 138302.
- [19] M. E. DMello, N. G. Sundaram, and S.B. Kalidindi, *Chem. Eur. J.*, 2018, **24**, 9220.
- [20] H. Tian, H. Fan, M. Li, and L. Ma, *ACS sensors*, 2016, **1**, 243.
- [21] Y. Lv, P. Xu, H. Yu, J. Xu, and X. Li, *Sens. Actuators B Chem.*, 2018, **262**, 562.
- [22] V. Chernikova, O. Yassine, O. Shekhah, M. Eddaoudi, and K.N. Salama, *J. Mater. Chem. A.*, 2018, **6**, 5550.

- [23] A. H. Assen, O. Yassine, O. Shekhah, M. Eddaoudi, and K.N. Salama, *ACS sensors*, 2017, **2**, 1294.
- [24] Z. Sun, S. Yu, L. Zhao, J. Wang, Z. Li, and G. Li, *Chem. Eur. J.*, 2018, **24**, 10829.
- [25] K. Guo, L. Zhao, S. Yu, W. Zhou, Z. Li, and G. Li, *Inorg. Chem.*, 2018, **57**, 7104.
- [26] T. Xu, P. Xu, D. Zheng, H. Yu, and X. Li, *Anal. Chem.*, 2016, **88**, 12234.
- [27] S. Homayoonnia, and S. Zeinali, *Sens. Actuators B Chem.*, 2016, **237**, 776.
- [28] K. Sel, S. Demirci, O. F. Ozturk, N. Aktas, and N. Sahiner, *Microelectron. Eng.*, 2015, **136**, 71.